CONTRAST MEDIA & MOLECULAR IMAGING
Contrast Media Mol Imaging **1**:259–266 (2006)
Published online 22 November 2006 in Wiley InterScience (www.interscience.wiley.com) DOI:10.1002/cmmi.113

CONTRAST MEDIA & MOLECULAR IMAGING

Full Paper

Targeted ultrasound contrast agent for molecular imaging of inflammation in high-shear flow

A. L. Klibanov, J. J. Rychak, W. C. Yang, S. Alikhani, B. Li, S. Acton, J. R. Lindner, K. Ley and S. Kaul*

University of Virginia, Charlottesville, VA 22908-0158, USA

Received 1 January 2006; Revised 5 October 2006; Accepted 6 October 2006

ABSTRACT: Targeted ultrasound contrast materials (gas-filled microbubbles carrying ligands to endothelial selectins or integrins) have been investigated as potential molecular imaging agents. Such microbubbles normally exhibit good targeting capability at the slower flow conditions. However, in the conditions of vigorous flow, binding may be limited. Here, we describe a microbubble capable of efficient binding to targets both in slow and fast flow (exceeding 4 dyne/cm^2 wall shear stress) using a clustered polymeric form of the fast-binding selectin ligand sialyl Lewis^X. Microbubbles were prepared from decafluorobutane gas and stabilized with a monolayer of phosphatidylcholine, PEG stearate and biotin-PEG-lipid. Biotinylated PSLe^x (sialyl Lewis^X polyacrylamide) or biotinylated anti-P-selectin antibody (RB40.34) was attached to microbubbles via a streptavidin bridge. In a parallel plate flow chamber targeted adhesion model, PSLe^x bubbles demonstrated specific adhesion, retention and slow rolling on P-selectin-coated plates. Efficiency of firm targeted adhesion to a P-selectin surface (140 molecules/μm^2) was comparable for antibody-carrying bubbles and PSLe^x-targeted bubbles at 0.68 dyne/cm^2 shear stress. At fast flow (4.45 dyne/cm^2), PSLe^x-targeted bubbles maintained their ability to bind, while antibody-mediated targeting dropped more than 20-fold. At lower surface density of P-selectin (7 molecules/μm^2), targeting via PSLe^x was more efficient than via antibody under all the flow conditions tested. Negative control casein-coated plates did not retain bubbles in the range of flow conditions studied. To confirm echogenicity, targeted PSLe^x-bubbles were visualized on P-selectin-coated polystyrene plates by ultrasound imaging with a clinical scanner operated in pulse inversion mode; control plates lacking targeted bubbles did not show significant acoustic backscatter. *In vivo*, in a murine model of inflammation in the femoral vein setting, targeting efficacy of intravenously administered PSLe^x-microbubbles was comparable with targeting mediated by anti-P-selectin antibody, and significantly exceeded the accumulation of non-targeted control bubbles. In the inflamed femoral artery setting, PSLe^x-mediated microbubble targeting was superior to antibody-mediated targeting. Copyright © 2006 John Wiley & Sons, Ltd.

KEYWORDS: microbubbles; targeting; echo contrast; ultrasound contrast; P-selectin; inflammation; ultrasound imaging; sialyl Lewis^X

INTRODUCTION

Ultrasound contrast agents carrying targeting ligands on the particle surface have been suggested as selective imaging agents for the detection and evaluation of intravascular pathology, including thrombosis (1), inflammation (2,3), ischemia–reperfusion injury (3), transplant rejection (4), tumor angiogenesis (5,6) or therapeutic angiogenesis (7). The design of targeted contrast particles can be a multilayer liposome (8), a liquid fluorocarbon particle (9), or a gas-filled microbubble (10). Gas-filled particles possess an excellent acoustic backscatter response; ultrasound imaging is capable of detection of individual micron-size particles (picogram level detection sensitivity) (10). Microparticle contrast agents are often targeted to specific molecular markers of disease using monoclonal antibodies, which have been shown to exhibit good targeting capability in slow and medium flow conditions (not exceeding 1 dyne/cm^2 shear stress, equivalent to a near-wall particle velocity $\sim$100 μm/s) (11). Such conditions can be found at the venous side of the microcirculation. However, in the conditions of higher shear flow, such as those found in arteries, these antibody-targeted bubbles may not adhere to the target efficiently (11). Therefore, we sought to devise targeted

**Correspondence to*: A. L. Klibanov, Cardiovascular Division, University of Virginia School of Medicine, Hospital Drive, Cobb Hall, RM 1026, Charlottesville, VA 22908/0158, USA.
E-mail: ALK6N@virginia.edu
Contract/grant sponsor: NIH Cardiovascular Training Grant; *contract/grant number:* HL07284.
Contract/grant sponsor: NIH; *contract/grant numbers:* DK63508 and HL64381; BRP EB002185.
Contract/grant sponsor: Philips Ultrasound Research.

Abbreviations used: PSLe^x, Sialyl Lewis^x polyacrylamide; DPBS, Dulbecco's phosphate-buffered saline.

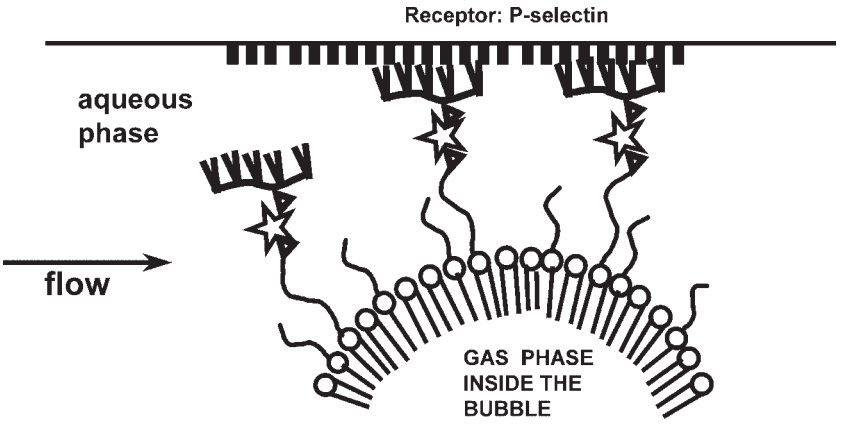

Figure 1. Design of the targeted microbubble construct and parallel plate flow chamber targeting experiment. Triangles, biotin residues; stars, streptavidin molecules; angles, SLe^x residues.

microbubble preparations capable of targeting in a wide variety of the flow conditions that may exist within the vasculature.

In this study we design and evaluate microbubble contrast material capable of binding to targets in fast flow (exceeding 4 dyne/cm^2 shear stress, or a particle velocity of ~390 μm/s), using a clustered polymeric form of the fast-binding selectin ligand sialyl Lewis^x ($PSLe^x$) (Figure 1). Particles bearing sialyl Lewis oligosaccharides are known to associate selectively and rapidly with P- or E-selectins (12–15); however, the overall affinity of sialyl Lewis to these selectins is generally not very high (16); oligo- or polymeric variants of this ligand have been shown to attach to selectins more efficiently than individual molecules (17,18). The monomeric form of sialyl Lewis^X has been tested recently as a microbubble targeting agent in a dual-targeting setting, in combination with anti-ICAM-1 antibody (19). As the targeting efficacy of the polymeric form of this ligand is superior to that of the monomer, it may facilitate the design of an efficient inflammation-targeted molecular imaging microbubble preparation that can be easily assembled from available components.

RESULTS

Targeting efficacy: parallel plate flow system

In the parallel plate flow chamber setting (Figure 1), both antibody-targeted and $PSLe^x$-carrying bubbles demonstrated selective accumulation and retention on P-selectin-coated plates. Control plates, coated only with casein blocker solution, did not retain bubbles in the range of the flow conditions studied (bubbles passed through the region of interest without stopping). Firm adhesion efficiency of targeting to the P-selectin surface (140 molecules/μm^2) was comparable for antibody-carrying bubbles and $PSLe^x$-carrying bubbles at 0.68 dyne/cm^2 shear stress (calculated near-wall particle velocity of 67 μm/s). As the flow rate and wall shear stress in the flow chamber were increased, antibody-mediated and $PSLe^x$-mediated targeting efficacy behaved in a different manner. Antibody-mediated targeting gradually decreased, and at 4.45 dyne/cm^2 (particle velocity of 438 μm/s) it dropped more than 20-fold, while $PSLe^x$-targeted bubbles maintained their ability to firmly bind to the target (Figure 2). The fraction of time the attached bubbles remained stationary on the target surface exceeded 95–99%.

At lower density of P-selectin on the target surface (7 molecules/μm^2), antibody-mediated targeting was consistently inferior to $PSLe^x$-mediated targeting of microbubbles in all the flow conditions studied (Figure 3).

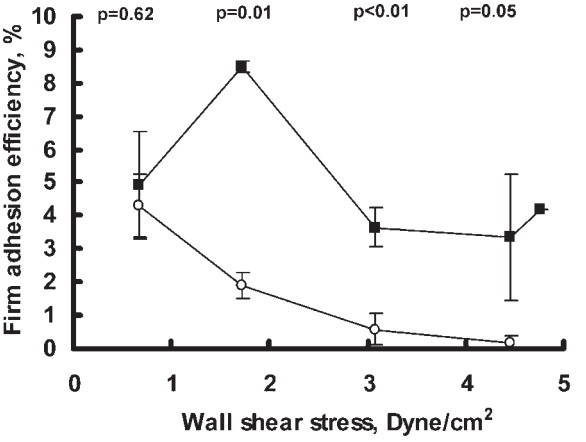

Figure 2. Efficacy of firm adhesion of targeted microbubbles to P-selectin-coated polystyrene surface in a parallel plate flow chamber (140 molecules/μm^2). Dependence on wall shear stress. Circles, RB40.34 antibody-carrying bubbles; squares, $PSLe^x$ carrying bubbles. Mean ± SEM (all experiments performed in triplicate).

DOI: 10.1002/cmmi

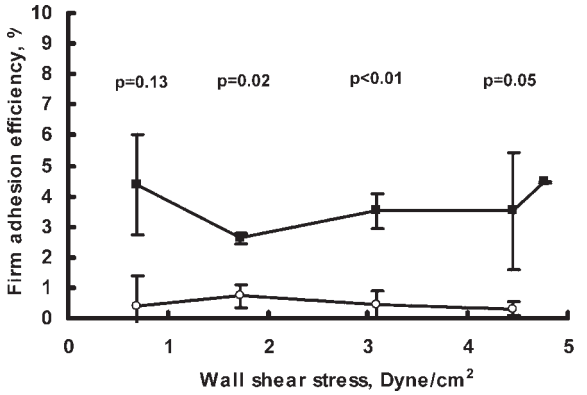

Figure 3. Efficacy of firm adhesion of targeted microbubbles to P-selectin-coated polystyrene surface in a parallel plate flow chamber (7 molecules/μm^2). Dependence on wall shear stress. Circles, RB40.34 antibody-carrying bubbles; squares, $PSLe^x$ carrying bubbles. Mean ± SEM (all experiments performed in triplicate).

Ultrasound imaging of targeted microbubbles

$PSLe^x$-microbubbles targeted to the area coated with P-selectin on the surface of polystyrene dish were selectively attaching to this area and not to the control surface coated only with casein blocker solution (Figure 4). Selective targeting in this static system was confirmed by microscopy: microbubbles were attached to the marked area that was coated with P-selectin, and not the control area. The microbubble-carrying P-selectin spot (~1 cm in diameter) was selectively visualized with the clinical grade ultrasound medical imaging system (Figure 5).

In vivo microbubble targeting: comparison of targeting ligands efficacy

The retention of microbubbles targeted with $PSLe^x$, RB40.34, or biotin alone was assessed by intravital microscopy in the large femoral vessels of mice pretreated with a local pro-inflammatory stimulus. The

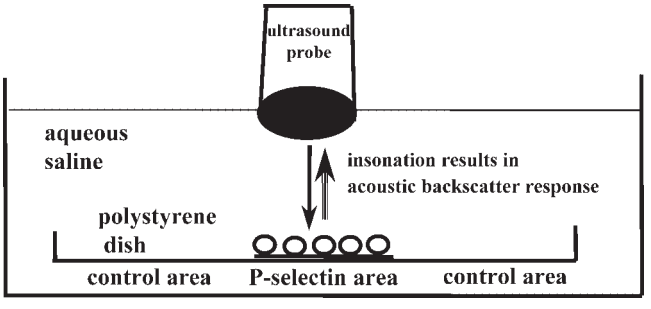

Figure 4. Ultrasound imaging of $PSLe^x$-targeted bubbles on the 35 mm Petri dish with P-selectin coated spot in the center: experimental design.

total intravascular area of all femoral vein segments analyzed in mice receiving microbubbles coupled to $PSLe^x$ ($0.64 \pm 0.25\,mm^2$), RB40.34 ($0.86 \pm 0.33\,mm^2$), or biotin alone ($0.80 \pm 0.17\,mm^2$) was not statistically different, nor was the total analyzed intravascular area of the femoral artery segments (0.53 ± 0.14, 0.67 ± 0.22, $0.48 \pm 0.03\,mm^2$, respectively).

In the inflamed femoral vein, microbubbles targeted with $PSLe^x$ or RB40.34 exhibited significantly greater retention than control microbubbles carrying biotin residues (Figure 6). There was no statistically significant difference in retention between microbubbles targeted with $PSLe^x$ and RB40.34 in this vessel. However, significantly higher retention of microbubbles targeted with $PSLe^x$ compared to RB40.34 was observed in the femoral artery ($p < 0.001$). The retention of negative control microbubbles bearing only biotin was low in both vessels.

DISCUSSION

Targeting of drug carrier systems, such as liposomes (20), polymers (17) and nano- and microparticles (21) to the biomolecules upregulated on the surface of vascular endothelium in areas of disease has been at the forefront of the development of targeted imaging. Targeting to P- or E-selectin (or to cell adhesion molecules such as ICAM-1) mimics the signaling that the human body uses in the leukocyte adhesion cascade to attract leukocytes to the areas of pathology (22). Targeted microbubbles directed to these receptors allow contrast enhancement imaging of these areas of interest. Antibody-coated bubbles (2,3) successfully show proof of principle in targeted ultrasound imaging. Monoclonal antibodies offer high affinity and specificity to the target antigens; however, they possess a number of disadvantages. Antibodies are expensive, and they can denature during storage or in the harsh conditions of bubble preparation. Unless humanized immunoglobulins are applied, antibodies can cause undesired immune response. Antibody molecules are bulky, so their density on the particle surface is limited. Most antibodies attach to their respective antigens firmly (i.e. complex dissociation rate is slow), but the association is not always fast (i.e. antigen–antibody complex formation on-rate kinetics tends to be slow) (23). If a particle (a cell or a microbubble) is rapidly moving through the blood vessel and has a limited time to interact with the vessel wall components, the rate of attachment of ligand to receptor becomes critical. For example, the velocity of a typical microbubble near the endothelium in a venule is on the order of 0.55 mm/s. Assuming a size of the target selectin molecule is ~30 nm, a microbubble has a limited time of about 0.06 ms to form a bond as it passes by the target. In nature, a set of specialized ligands has evolved to achieve fast attachment of leukocytes to activated endothelium,

DOI: 10.1002/cmmi

Figure 5. Ultrasound imaging of PSLe^x-targeted bubbles on the 35 mm petri dish with P-selectin coated spot in the center. Imaging performed with an HDI5000 system in the general pulse inversion mode at MI $\approx$ 0.1.

such as P-selectin glycoprotein ligand 1 (PSGL-1) or other sulfated, fucosylated and/or sialylated molecules (22).

A functional terminal glycosulfopeptide modeled on PSGL-1 has been isolated (16,24). This molecule is relatively small, $\sim$4 kDa, with equilibrium K_d in the sub-micromolar range, similar to PSGL-1. However, dissimilar to many antibodies, its rate of association with P-selectin is high (16). Targeting of microbubbles with this ligand in fast flow conditions has been efficient (25). However, the chemical synthesis, especially the proper placement of sulfate and SLe^x residues on the peptide chain, requires extensive technical skill. Simpler molecules (sialylated oligosaccharides, $\sim$1 kDa) are described in the literature as targeting ligands directed to P- or E-selectin. The main disadvantage of the most popular ligand of this class, sialyl Lewis^X, is its low binding affinity, with the equilibrium K_d in millimolar range (26). A known approach, use of cooperative multi-point binding via oligomerization of low-affinity ligands, can be applied to convert sialyl Lewis^X into a ligand with much higher overall avidity to the target-coated surface (17,18,27). A polymeric version of sialyl Lewis^X is available in biotinylated form, so the attachment of this ligand to microbubbles can be easily performed by the standard procedures (3,11,28). A copolymer of polyacrylamide with biotin–acrylate and sialyl Lewis^X acrylate is $\sim$30 kDa according to the manufacturer; from the provided ratio of acrylamide, biotin and SLe^x residues, one can compute that each polymer chain carries about 10 SLe^x residues and about two biotins.

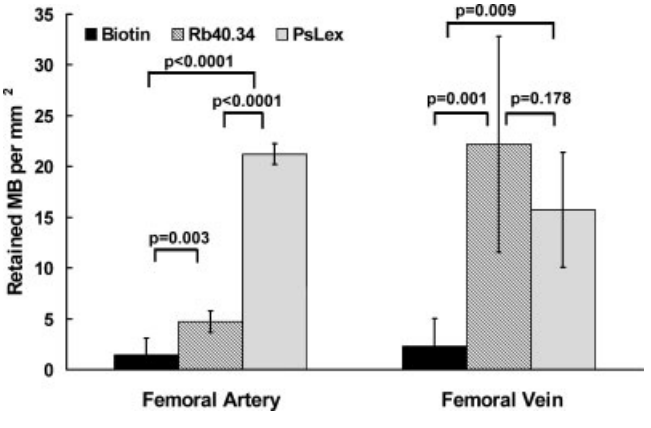

Figure 6. Intravital microscopy of firm adhesion of targeted fluorescent microbubbles in the exposed murine femoral vessels treated with TNF-α. Dotted bar, PSLe^x carrying bubbles; striped bar, RB40.34 antibody-carrying bubbles; dark bar, control biotinylated bubbles. Error bars represent standard deviation.

It is known that the retention of microbubbles on the target in fast shear flow conditions is benefited by increasing the concentration of ligands on the bubble surface (28,29). Typically, $\sim 10^5$ biotinylated antibody molecules are attached per microbubble by the standard streptavidin-biotin scheme (3,11,28). An order of magnitude higher number of SLe^x ligand molecules can be placed on the bubble surface even if we assume a simple 1:1 replacement of each antibody with a polymer molecule, which would result in 10-fold increase of the surface density of the ligand on the bubble shell, and an

DOI: 10.1002/cmmi

improved ability to target, due to the high-avidity cooperative multipoint interaction between the targeted particle and the receptor surface combined with fast-binding property of this ligand.

Indeed, $PSLe^x$-carrying microbubbles are shown by the experiments presented here to attach efficiently and firmly to P-selectin-coated surfaces; targeting efficacy by $PSLe^x$-microbubbles is superior to antibody-mediated targeting in fast flow conditions, especially in the case of lower surface density of P-selectin (Figures 2 and 3). Targeted $PSLe^x$-microbubbles were acoustically active (Figure 5) and serve as an efficient ultrasound contrast delineating receptor-coated surface. An *in vivo* fluorescence intravital microscopy study in mouse femoral vasculature showed that $PSLe^x$-microbubbles exhibited targeting efficacy comparable to anti-P-selectin antibody-coated microbubbles in the femoral vein. In the fast-flow conditions of femoral artery, $PSLe^x$-mediated targeting of microbubbles was superior to antibody-mediated targeting (Figure 6). Here, $PSLe^x$-microbubbles may be directed not only to P- but also to upregulated E-selectin molecules on the luminal surface of vascular endothelium. Interestingly, a monomeric form of SLe^x has been recently tested in a dual-targeting system, where targeted microbubbles carried at the same time SLe^x and anti-ICAM-1 antibody (19); apparently SLe^x is used to 'slow down' the bubbles, so that the antibody can subsequently achieve firm anchoring to ICAM-1. Perhaps a polymeric form of SLe^x with higher avidity to selectins would not require additional targeting ligands; a side-by-side comparison of SLe^x- and $PSLe^x$-carrying targeted microbubble preparations may be necessary to achieve better understanding of the adhesion events in high shear flow.

A significant advantage of the use of $PSLe^x$-targeted bubbles is the applicability to a wide variety of animal species. Unlike an antibody, which usually provides species-specific affinity (most popular are rat-generated antibodies against mouse selectins), $PSLe^x$ is known to interact with P-, E- and L-selectins of various species; therefore, these bubbles could be directly employed in a variety of *in vivo* targeted inflammation imaging protocols, from mice to larger animals, including humans.

Further studies should include testing of targeted contrast ultrasound imaging *in vivo*, especially in the conditions of high shear flow vasculature. Additional ligand modification may be helpful: while SLe^x or SLe^a are available molecules for targeting applications, a significant improvement in the binding affinity of Lewis oligosaccharides can be achieved by sulfation (30), bringing it in close range to PSGL-1 (24). Polymeric versions of the sulfated sialyl Lewis derivatives may further improve targeting. Direct covalent coupling of polymeric ligand clusters to the microbubble surface instead of streptavidin linker (an immunogenic foreign protein) may increase the targeting ligand concentration and lead to additional improvement of the targeting efficacy. For clinical use polyacrylamide may be substituted with a fully biodegradable polymer.

CONCLUSION

Polymeric sialyl $Lewis^X$, clustered on the surface of contrast agent particle in order to achieve high ligand surface density allows selective targeting of ultrasound contrast microbubbles on P-selectin coated surfaces. Binding in the fast flow conditions was considerably improved as compared with anti-P-selectin antibody-targeted bubbles. Targeted bubbles selectively delineated the area coated with P-selectin on the surface of polystyrene dish, and selectively attached to activated vascular endothelium *in vivo* in a murine femoral vasculature inflammation model.

EXPERIMENTAL

Microbubble preparation and targeting ligand attachment

Microbubbles were prepared from decafluorobutane gas and stabilized with a monolayer of distearoyl phosphatidylcholine, PEG stearate and biotin-PEG-lipid (31). Aqueous micellar dispersion of 2 mg/ml of phosphatidylcholine (Avanti Lipids, Alabaster, AL, USA), 1 mg/ml poly(ethylene glycol) 40 stearate (Sigma, St Louis, MO, USA), 0.1 mg/ml biotin-PEG3400-phosphatidylethanolamine (31) and, when necessary, a trace amount of DiI dye (Molecular Probes, Eugene, OR, USA) was sonicated with a probe-type sonicator XL2020 (Heat Systems/Misonix, Farmingdale, NY, USA) at maximum power in an atmosphere of decafluorobutane (Flura, Newport, TN, USA). As the gas was dispersed in the aqueous phase and microbubbles formed, they were immediately coated and stabilized with a self-assembled lipid/surfactant monolayer. Microbubbles were stored refrigerated in sealed vials in decafluorobutane atmosphere.

Biotinylated SLe^x polyacrylamide ($PSLe^x$, Glycotech, Rockville, MD, USA) or biotinylated anti-P-selectin antibody (RB40.34, positive control) (32) were attached to the microbubble surface via streptavidin (11). Microbubbles were washed with degassed Dulbecco's phosphate-buffered saline (DPBS, GIBCO/Invitrogen, Grand Island, NY, USA) five times in a bucket rotor centrifuge at $\sim 30\,\boldsymbol{g}$ for 4 min to remove excess unincorporated lipid from the microbubbles. Three micrograms of streptavidin (Sigma, St Louis, MO, USA) per 10^7 microbubbles was then added to the washed microbubble dispersion. Following 30 min of incubation on ice, the microbubbles were washed twice

DOI: 10.1002/cmmi

(same centrifugation conditions) to remove unreacted streptavidin, and incubated on ice with 7.5 μg of biotinylated anti-mouse P-selectin antibody RB40.34 (UVA Lymphocyte Culture Center, Charlottesville, VA, USA) per 10^7 microbubbles, or 1.5 μg of $PSLe^x$ (Glycotech, Rockville, MD, USA) for 30 min and washed in the centrifuge to remove free ligand. Bubble preparations were stored on ice under decafluorobutane atmosphere.

In vitro parallel plate flow studies.

In vitro testing of targeted adhesion was performed by video microscopy in the parallel plate flow chamber (11). The microbubble dispersion (10^7 particles per ml) in degassed DPBS buffer containing calcium and magnesium, was passed through a rectangular flow chamber (Glycotech, Rockville, MD, USA) formed by a 0.125 mm rubber gasket and Lucite block inserted in a 35 mm Petri dish. The Petri dish surface was coated with the murine P-selectin fusion protein (R&D Systems, Minneapolis, MN, USA) at surface densities of 7 or 140 molecules/μm^2(11). Control studies of nonspecific binding were performed with casein-blocked dishes. The microbubble dispersion was driven from a stirred cell via a short capillary into the flow chamber. A syringe pump operated in the withdrawal mode was connected to the exit of the flow chamber. The flow chamber assembly was positioned upside down and placed on the stage of Leitz Laborlux 11 microscope (Leica, Wetzlar, Germany) equipped with a $40\times$ long working distance objective and a CCD video camera (NTSC). A single field of view (110×150 μm) in the center of the flow deck was followed by video microscopy for the duration of each flow experiment. The flow chamber was observed under brightfield transillumination microscopy. It enabled discrimination between targeted bubbles that firmly attached to P-selectin layer, bubbles that rolled across the target surface at a velocity less than free-stream, bubbles that paused on the target surface temporarily, and bubbles that traversed the imaging frame at free-stream velocity. Video microscopy data was recorded on miniDV cassettes. iMovie software was used to extract the video files, which were converted into avi format. Microbubble flux, targeting efficacy, rolling velocity and pause times were computed using a novel image processing software based on Matlab package (33). Microbubble adhesion was classified as firm if the bubbles remained at their location for over 5 s. To compute the adhesion efficacy, the number of adherent microbubbles was divided by the flux of microbubbles traversing by the target surface. This parameter takes into account potential differences in the delivery of the microbubbles of various preparations to the target surface. Microbubble translational velocity was calculated according to Goldman *et al.* (34).

Intravital microscopy

The animal protocol was approved by the UVA Institutional Animal Care and Use Committee. Intravital microscopy was performed in a model of inflammation of the mouse hindleg (35,36). The retention of microbubbles bearing $PSLe^x$ ($n=5$ mice), the monoclonal antibody RB40.34 ($n=4$ mice) or biotin alone ($n=5$ mice) was assessed in inflamed femoral vein and artery segments of C57Bl/6 mice (Hilltop Lab Animals, Scottsdale, PA, USA) between the ages of 8 and 12 weeks. P-selectin expression at the vascular endothelium was induced by pretreatment with 500 ng murine TNF-α (R&D Systems, Minneapolis, MN, USA), injected into the plantar surface of the hind paw three hours before microbubble administration (35). Mice were anesthetized with an intraperitoneal injection of 125 mg/kg body weight ketamine (Ford Dodge Animal Health, Ford Dodge, IA, USA), 12.5 mg/kg body weight xylazine (Burns Veterinary Supply, Westbury, NY, USA), and 0.025 mg/kg body weight atropine sulfate (American Pharmaceutical Partners, Schaumburg, IL, USA). Body temperature was maintained at 38 °C during preparation with a heat pad. Trachea intubation to promote respiration was accomplished with PE 90 tubing (Beckton Dickinson, Franklin Lakes, NJ, USA), and the right jugular vein was cannulated with PE 20 tubing (Beckton Dickinson) for administration of microbubbles.

The anesthetized mouse was placed prone on the heated microscope stage, and the hindleg secured. The skin on the inside hindleg surface was retracted to expose the femoral vessels and superfused with an isothermic bicarbonate-buffered solution (37). The femoral vessels were visualized by fluorescence microscopy using a saline immersion objective (Zeiss SW 40/0.8 NA) and a CCD camera (Hamamatsu 2400, Hamamatsu, Shizuoka, Japan). Video was recorded onto VHS videocassettes for off-line analysis. DiI-microbubbles bearing $PSLe^x$, RB40.34, or biotin alone were administered as a bolus of 5×10^6 particles in 150 μl saline through the jugular cannula, followed by a 25 μl saline flush. Microbubble retention within the femoral vein or artery was assessed in 10–20 fields of view 5–10 min after microbubble administration. The total intravascular area of each femoral vein and artery segment and the number of retained microbubbles was determined off-line by a reviewer blinded to the nature of the administered sample. Statistical significance was tested using one-way ANOVA followed by the Bonferroni post-test, as appropriate. Error bars on the figures represent the standard deviation.

Static binding and ultrasound imaging of targeted microbubbles

Static binding and ultrasound imaging of targeted microbubbles were performed (38). A dispersion of

DOI: 10.1002/cmmi

$\sim 10^7$ microbubbles in 10 ml DPBS with calcium and magnesium was placed in 35 mm Petri dishes, where a center 1 cm spot was coated with P-selectin as described above. The dishes were sealed, inverted, incubated for 15 min, seal was removed and free bubbles that did not attach to the target were removed by a DPBS rinse. The dishes were then placed in the aqueous environment and ultrasound imaging with a clinical HDI5000 system (Philips, Bothell, WA, USA) was performed with a L7-4 probe (Figures 4 and 5). The system was operated in the intermittent general pulse inversion mode, with low mechanical index ($\sim$0.1) to avoid destruction of microbubbles. The dishes were positioned at an angle different from perpendicular to the transducer axis to avoid specular reflection from plastic.

Acknowledgements

A.L. Klibanov is grateful to UVA Cardiovascular Division, Robert M. Berne Cardiovascular Research Center and Cardiovascular Imaging Center for help and support. A generous donation of laboratory equipment to A.L. Klibanov's laboratory at UVA Cardiovascular Division by Mallinckrodt Inc. (St Louis, MO, USA) is appreciated. J.J. Rychak was supported via NIH Cardiovascular training grant HL07284 to UVA. J.R. Lindner was supported in part via NIH DK63508 and HL64381. A.L. Klibanov is grateful to Philips Ultrasound Research for support and for making the HDI5000 scanner available. This study was supported in part via NIH BRP EB002185 to K. Ley.

REFERENCES

1. Unger E, Metzger P, Krupinski E, Baker M, Hulett R, Gabaeff D, Mills J, Ihnat D, McCreery T. The use of a thrombus-specific ultrasound contrast agent to detect thrombus in arteriovenous fistulae. *Invest. Radiol.* 2000; **35**: 86–89.
2. Villanueva FS, Jankowski RJ, Klibanov S, Pina ML, Alber SM, Watkins SC, Brandenburger GH, Wagner WR. Microbubbles targeted to intercellular adhesion molecule-1 bind to activated coronary artery endothelial cells. *Circulation* 1998; **98**: 1–5.
3. Lindner JR, Song J, Christiansen J, Klibanov AL, Xu F, Ley K. Ultrasound assessment of inflammation and renal tissue injury with microbubbles targeted to P-selectin. *Circulation* 2001; **104**: 2107–2112.
4. Weller GER, Lu E, Csikari MM, Klibanov AL, Fischer D, Wagner WR, Villanueva FS. Ultrasound Imaging of acute cardiac transplant rejection with microbubbles targeted to intercellular adhesion molecule-1. *Circulation* 2003; **108**: 218–224.
5. Ellegala DB, Leong Poi H, Carpenter JE, Klibanov AL, Kaul S, Shaffrey ME, Sklenar J, Lindner JR. Imaging tumor angiogenesis with contrast ultrasound and microbubbles targeted to alpha(v)-beta(3). *Circulation* 2003; **108**: 336–341.
6. Weller GER, Wong MKK, Modzelewski RA, Lu EX, Klibanov AL, Wagner WR, Villanueva FS. Ultrasonic imaging of tumor angiogenesis using contrast microbubbles targeted via the tumor-binding peptide arginine-arginine-leucine. *Cancer Res.* 2005; **65**: 533–539.
7. Leong-Poi H, Christiansen J, Heppner P, Lewis CW, Klibanov AL, Kaul S, Lindner JR. Assessment of endogenous and therapeutic arteriogenesis by contrast ultrasound molecular Imaging of integrin expression. *Circulation* 2005; **111**: 3248–3254.
8. Demos SM, Onyuksel H, Gilbert J, Roth SI, Kane B, Jungblut P, Pinto JV, McPherson DD, Klegerman ME. *In vitro* targeting of antibody-conjugated echogenic liposomes for site-specific ultrasonic image enhancement. *J. Pharm. Sci.* 1997; **86**: 167–171.
9. Lanza GM, Trousil RL, Wallace KD, Rose JH, Hall CS, Scott MJ, Miller JG, Eisenberg PR, Gaffney PJ, Wickline SA. *In vitro* characterization of a novel, tissue-targeted ultrasonic contrast system with acoustic microscopy. *J. Acoust. Soc. Am.* 1998; **104**: 3665–3672.
10. Klibanov AL, Rasche PT, Hughes MS, Wojdyla JK, Galen KP, Wible JH, Brandenburger GH. Detection of individual microbubbles of ultrasound contrast agents—imaging of free-floating and targeted bubbles. *Invest. Radiol.* 2004; **39**: 187–195.
11. Takalkar AM, Klibanov AL, Rychak JJ, Lindner JR, Ley K. Binding and detachment dynamics of microbubbles targeted to P-selectin under controlled shear flow. *J. Control Release* 2004; **96**: 473–482.
12. Goetz DJ, Greif DM, Ding H, Camphausen RT, Howes S, Comess KM, Snapp KR, Kansas GS, Luscinskas FW. Isolated P-selectin glycoprotein ligand-1 dynamic adhesion to P- and E-selectin. *J. Cell Biol.* 1997; **137**: 509–519.
13. Rodgers SD, Camphausen RT, Hammer DA. Sialyl Lewis(x)-Mediated, PSGL-1-independent rolling adhesion on P-selectin. *Biophys. J.* 2000; **79**: 694–706.
14. Brunk DK, Goetz DJ, Hammer DA. Sialyl Lewis(x)/E-selectin-mediate rolling in a cell-free system. *Biophys. J.* 1996; **71**: 2902–2907.
15. Brunk DK, Hammer DA. Quantifying rolling adhesion with a cell-free assay: E-selectin and its carbohydrate ligands. *Biophys. J.* 1997; **72**: 2820–2833.
16. Yago T, Leppanen A, Qiu HY, Marcus WD, Nollert MU, Zhu C, Cummings RD, McEver RP. Distinct molecular and cellular contributions to stabilizing selectin-mediated rolling under flow. *J. Cell Biol.* 2002; **158**: 787–799.
17. WeitzSchmidt G, Stokmaier D, Scheel G, Nifantev NE, Tuzikov AB, Bovin NV. An E-selectin binding assay based on a polyacrylamide-type glycoconjugate. *Anal. Biochem.* 1996; **238**: 184–190.
18. Stahn R, Schafer H, Kernchen F, Schreiber J. Multivalent sialyl Lewis x ligands of definite structures as inhibitors of E-selectin mediated cell adhesion. *Glycobiol.* 1998; **8**: 311–319.
19. Weller GER, Villanueva FS, Tom EM, Wagner WR. Targeted ultrasound contrast agents: In vitro assessment of endothelial dysfunction and multi-targeting to ICAM-1 and sialyl Lewis. *Biotechnol. Bioeng.* 2005; **92**: 780–788.
20. Zalipsky S, Mullah N, Harding JA, Gittelman J, Guo L, DeFrees SA. Poly(ethylene glycol)-grafted liposomes with oligopeptide or oligosaccharide ligands appended to the termini of the polymer chains. *Bioconjug. Chem.* 1997; **8**: 111–118.
21. Eniola AO, Hammer DA. *In vitro* characterization of leukocyte mimetic for targeting therapeutics to the endothelium using two receptors. *Biomaterials* 2005; **26**: 7136–7144.
22. Ley K. The role of selectins in inflammation and disease. *Trends Mol. Med.* 2003; **9**: 263–268.
23. Chen SQ, Alon R, Fuhlbrigge RC, Springer TA. Rolling and transient tethering of leukocytes on antibodies reveal specializations of selectins. *Proc. Natl Acad. Sci. USA* 1997; **94**: 3172–3177.
24. Leppanen AM, McEver RP, Cummings RD. Synthesis of a novel glycosulfopeptide that binds to P-selectin with high affinity and inhibits leukocyte adhesion to P-selectin. *Glycobiology* 1999; **9**: 1143–1144.
25. Rychak JJ, Klibanov AL, Leppanen A, Cummings RD, Ley K. Enhanced binding of ultrasound contrast microbubbles targeted to P-selectin using a physiological capture ligand. *Faseb J.* 2004; **18**: A446–A446.
26. Beauharnois ME, Lindquist KC, Marathe D, Vanderslice P, Xia J, Matta KL, Neelamegham S. Affinity and kinetics of sialyl Lewis-X and core-2 based oligosaccharides binding to L- and P-selectin. *Biochem.* 2005; **44**: 9507–9519.
27. Ushakova NA, Preobrazhenskaya ME, Bird MI, Priest R, Semenov AV, Mazurov AV, Nifantiev NE, Pochechueva TV, Galanina OE, Bovin NV. Monomeric and multimeric blockers of selectins:

Comparison of in vitro and in vivo activity. *Biochemistry Moscow* 2005; **70**: 432–439.
28. Weller GER, Klibanov AL, Wagner WR, Villanueva FS. Variable antibody density on contrast microbubbles modulates targeted adhesion to dysfunctional endothelium. *Circulation* 2001; **104**(suppl): 352.
29. Klibanov AL, Hughes MS, Villanueva FS, Jankowski RJ, Wagner WR, Wojdyla JK, Wible JH, Brandenburger GH. Targeting and ultrasound imaging of microbubble-based contrast agents. *Magma* 1999; **8**: 177–184.
30. Mowery P, Yang ZQ, Gordon EJ, Dwir O, Spencer AG, Alon R, Kiessling LL. Synthetic glycoprotein mimics inhibit L-selectin-mediated rolling and promote L-selectin shedding. *Chem. Biol.* 2004; **11**: 725–732.
31. Klibanov AL, Gu H, Wojdyla JK, Wible JH Jr, Kim DH, Needham D, Villanueva FS, Brandenburger GH. Attachment of ligands onto the gas-filled microbubbles via PEG spacer arm and lipid residues anchored at the interface. Proceedings of 26th International Symposium on Controlled Release of Bioactive Materials, Boston, Controlled Release Society, 1999; 124–125.
32. Bosse R, Vestweber D. Only Simultaneous blocking of the L-selectin and P-selectin completely inhibits neutrophil migration into mouse peritoneum. *Eur. J. Immunol.* 1994; **24**: 3019–3024.
33. Ray N, Acton ST, Ley K. Tracking leukocytes *in vivo* with shape and size constrained active contours. *IEEE Trans. Med. Imag.* 2002; **21**: 1222–1235.
34. Goldman AJ, Cox RG, Brenner H. Slow viscous motion of a sphere parallel to a plane wall—II Couette flow. *Chem. Engng Sci.* 1967; **22**: 653–660.
35. Eriksson EE, Xie X, Werr J, Thoren P, Lindbom L. Importance of primary capture and L-selectin dependent secondary capture in leukocyte accumulation in inflammation and atherosclerosis *in vivo*. *J. Exp. Med.* 2001; **194**: 205–218.
36. Schramm R, Menger MD, Schaefers H-J, Thorlacius H. Leukocyte adhesion in aorta and femoral artery in vivo is mediated by LFA-1. *Inflamm. Res.* 2004; **53**: 523–527.
37. Ley K, Bullard DC, Arbones ML, Bosse R, Vestweber D, Tedder TF, Beaudet AL. Sequential contribution of L-selectin and P-selectin to leukocyte rolling *in vivo*. *J. Exp. Med.* 1995; **181**: 669–675.
38. Klibanov AL, Hughes MS, Marsh JN, Hall CS, Miller JG, Wible JH, Brandenburger GH. Targeting of ultrasound contrast material—an *in vitro* feasibility study. *Acta Radiol.* 1997; **38**: 113–120.

DOI: 10.1002/cmmi